A Multi-MHz IPT-link Developed for Load Characterisation at Highly Variable Coupling Factor

Juan M. Arteaga, Lingxin Lan, Samer Aldhaher, George Kkelis, David C. Yates and Paul D. Mitcheson
Department of Electrical and Electronic Engineering
Imperial College London
j.arteaga-saenz15@imperial.ac.uk

***Abstract*—This paper presents the development and characterisation of an inductive link to assess and compare inductive power transfer (IPT) systems that operate at 6.78 or 13.56 MHz. First, the properties of two equal air-core coils were obtained from simulations and corroborated experimentally. Then, the coupling factor between the coils was calculated in function of separation and misalignment. A receiving-end circuit, comprised of a capacitance and a resistive load, was also characterised in order to reflect different loads to the transmitter at different tunings and couplings, and therefore represent the effects produced by changes in coupling and variations in the rectifier's input impedance. The link was tested, firstly using a Class E inverter and then a load-independent Class EF inverter, both at power levels lower than 200 W. The reflected load was changed by altering coupling, and the tuning capacitance. A comparison between these inverter topologies handling highly reactive loads is shown here for the first time.**

I. Introduction

A two coil IPT system can be modelled as two separate circuits, shown in Fig. 1, where the coils are linked by the coupling factor (k):

$$k = \frac{M_{\mathrm{ps}}}{\sqrt{L_{\mathrm{p}} L_{\mathrm{s}}}}. \tag{1}$$

Here L_{p} and L_{s} are the respective self inductances of the transmitting and receiving coils, and M_{ps} is the mutual inductance.

When no magnetically permeable materials are used to direct the magnetic flux in an IPT-link, k strictly depends on the alignment and separation of the coils [1], and therefore granting spatial freedom to the load entails operating at a broad range in k. Systems using multiple air-core coils, e.g. [2], [3], can operate at narrower ranges in k whilst granting spatial freedom, however requiring multiple transmitting coils and drive circuits is inconvenient. Operating at broad ranges in k is challenging not only because changes in coupling can severely affect the end-to-end efficiency of the system, but because regulating the output power, which is necessary in most applications, also produces changes on the input resistance and reactance of the rectifier at the receiving end [4].

Very few multi-MHz IPT systems capable of operating efficiently at broad ranges of k whilst having a regulated output power can be found in literature. For example, in our previous works [5], [6], we presented a drone without a battery that can hover over a $13.56\,\mathrm{MHz}$ IPT charging pad at a range of motion corresponding to a range of k of $5\,\%$ to $20\,\%$. An interesting feature of that case study is that the only control loop present in the system is the one of the dc-dc converter, used as the last stage of power conversion in the receiver. The dc-dc converter automatically changes its input resistance, and consequently the input impedance of the rectifier, when changes in demand or in k take place.

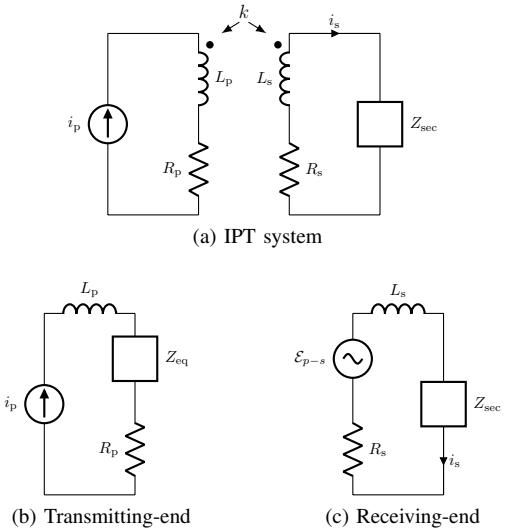

(a) IPT system

(b) Transmitting-end (c) Receiving-end

Fig. 1. Equivalent circuits of an IPT system.

The form in which the input impedance of the rectifier changes with load and k depends on the topology and design of the rectifier. Class E rectifiers can be designed with the necessary features to handle these sorts of conditions (broad changes in k and load demand) by tuning the passives at a frequency different than the system's operating frequency, and then tuning out the residual reactance of the rectifier in the resonant tank of the receiving-end [7]. This technique, however, relies on not only altering the rectifier's input resistance to regulate power as coupling or the load changes, but also on varying the input reactance, which can slightly detune the receiving-end circuit and therefore reflect a reactive load to the transmitter. This phenomenon is not exclusive to loads that use Class E rectifiers. Other sorts of loads, e.g. inductively coupled plasma [8], will tend to reflect a significant reactive component to the power transmitter. Also, foreign objects tend to reflect highly reactive impedances to the transmitter, which if well characterised, can be used as a foreign object detection mechanism.

Citation: J. M. Arteaga, L. Lan, S. Aldhaher, G. Kkelis, D. C. Yates and P. D. Mitcheson, "A Multi-MHz IPT-link Developed for Load Characterisation at Highly Variable Coupling Factor," 2018 IEEE Wireless Power Transfer Conference (WPTC), 2018, pp. 1-4. DOI: 10.1109/WPT.2018.8639239. IEEExplore link: https://ieeexplore.ieee.org/abstract/document/8639239

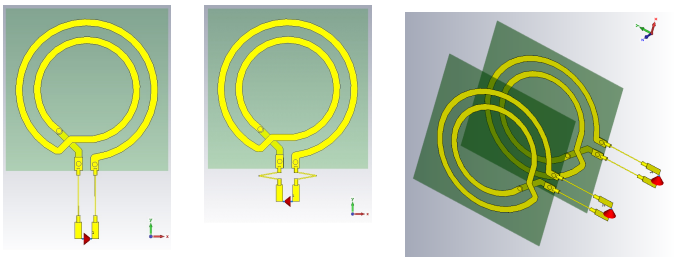

(a) Case 1: $L_{\min}$ (b) Case 2:$L_{\max}$ (c) Coupling simulations

Fig. 2. PCB coils modelled using CST.

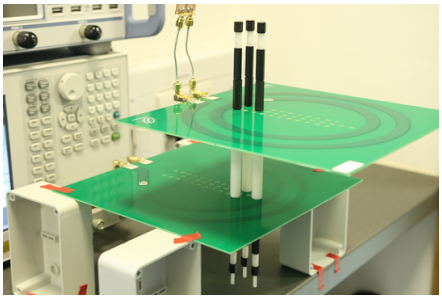

Fig. 3. Photograph of the coils and set-up to measure coupling.

II. Characterisation of an IPT-link

In order to tune the circuits at both ends of the system, it is necessary to obtain measurements on inductance and equivalent resistance of the IPT coils. We designed two equal printed-circuit-board coils with eleven sets of mounting holes in order to fix and reproduce an accurate link configuration, and then compare inverters and rectifiers using not only the same set of coils but the same link geometry. The designed coils can be seen in Figs. 3 and 6.

A. Coil Inductance and Equivalent Series Resistance

In order to characterise the coils, we performed 3D full-wave electromagnetic simulations considering different scenarios, as for example shown in Fig. 2, where different positions in the wires linking the circuit boards and the coils are considered. The simulation results can be verified using an impedance analyser (we use a Keysight E4990A), however the equivalent resistance of the coils is difficult to measure accurately at high Q factors [9]. The results of these measurements are shown in Table I.

TABLE I
Simulation and measurements of the coils at 13.56 MHz

Description	Inductance (nH)	Resistance (mΩ)	Q factor
Simulation at case 1: $L_{\min}$	1155.7	191.2	515
Simulation at case 2: $L_{\max}$	1200.4	189.2	541
Measurement at case 1: $L_{\min}$	1181.0	202.7	496
Measurement at case 2: $L_{\max}$	1185.2	227.2	444

B. Coupling Simulations and Measurements

Once the coils have been characterised, the coupling between them can be calculated for different relative positions. 3D electromagnetic simulations were performed to determine coupling at coil separation distances ranging from 10 mm to 250 mm and linear misalignments from 0 mm to 250 mm. These results were also verified using an impedance analyser.

C. Development and Characterisation of an ac-Load

A circuit comprised of a capacitance and a resistance was designed and built to provide a well tuned and measurable inductively powered load to an IPT transmitter under test. The load consists of twelve resistors of 100 Ω (LTO100F15R00JTE3) in parallel, resulting in a total resistance of 8.41 Ω, measured at 13.56 MHz, where no significant variations in resistance were detected as temperature increased. This resistance guarantees a loaded-Q higher than 10 with the proposed coils at 13.56 MHz.

The resonant tank of the receiving-end was carefully tuned by fixing the coupling between the transmitting and receiving coils at 5 % and then adjusting the series capacitance of the receiving-end circuit whilst measuring the equivalent series resistance in the transmitting coil using an impedance analyser. The resonant frequency of the receiving-end circuit is determined by the maximum series resistance measured in the transmitting end. It should be mentioned that this technique is not effective to tune a circuit with a rectifier since the equivalent capacitance of diodes and transistors is highly dependent on voltage.

The proposed load circuit can be seen, attached to the receiving coil, in Fig. 6.

III. Case Study: Reflecting a Reactive Load to a Single Switch Inverter

When an IPT system is represented as the two circuits in Fig. 1, changes in coupling and in the variables used to regulate power account for changes in the following parameters: the output current of the inverter (i_{p}), the reflected impedance to the transmitter (Z_{eq}), the induced electromotive force at the receiving-end coil ($\mathcal{E}_{\mathrm{p-s_{rms}}}$) and the input impedance of the rectifier (Z_{sec}). These cover all the variables that are not intrinsic of the coils. For this analysis we consider the frequency of i_{p} ($f_{\mathrm{i_p}}$) to be constant, and Z_{sec} and the magnitude of the output current of the inverter ($i_{\mathrm{p_{rms}}}$) as variables for regulation against k. The equations that represent how these variables are formulated considering $\boldsymbol{Z_{\mathrm{sec}}} = R_{\mathrm{sec}} + \boldsymbol{j}X_{\mathrm{sec}}$, and $\boldsymbol{Z_{\mathrm{eq}}} = R_{\mathrm{eq}} + \boldsymbol{j}X_{\mathrm{eq}}$, are:

$$R_{\mathrm{eq}} = \frac{4\pi^2 f_{\mathrm{ip}}^2 k^2 L_{\mathrm{p}} L_{\mathrm{s}} \left(R_{\mathrm{s}} + R_{\mathrm{sec}}\right)}{\left(R_{\mathrm{s}} + R_{\mathrm{sec}}\right)^2 + \left(2\pi f_{\mathrm{i_p}} L_{\mathrm{s}} + X_{\mathrm{sec}}\right)^2}, \qquad (2)$$

$$X_{\mathrm{eq}} = -\frac{4\pi^2 f_{\mathrm{i_p}}^2 k^2 L_{\mathrm{p}} L_{\mathrm{s}} \left(2\pi f_{\mathrm{i_p}} L_{\mathrm{s}} + X_{\mathrm{sec}}\right)}{\left(R_{\mathrm{s}} + R_{\mathrm{sec}}\right)^2 + \left(2\pi f_{\mathrm{i_p}} L_{\mathrm{s}} + X_{\mathrm{sec}}\right)^2}, \tag{3}$$

and on the secondary side:

$$\boldsymbol{\mathcal{E}}_{\mathbf{p-s_{rms}}} = 2\pi f_{\mathrm{i_p}} k \sqrt{L_{\mathrm{p}} L_{\mathrm{s}}} \boldsymbol{i}_{\mathbf{prms}}. \tag{4}$$

These equations, which are practical for the design of the circuits at both ends if the operating frequency is constant, and k variable, can be derived from the circuits in Fig 1 or from the formulation presented in [10].

A. Characterisation of the Reflected Impedance

The proposed ac-load circuit was first tuned at the frequency of operation and then progressively detuned to also reflect a positive and negative reactance to the transmitter. The load was adjusted as shown in Table II.

TABLE II
LOADING CONDITIONS

Load	R_{sec} [Ω]	$2\pi f_{\mathrm{i_p}} L_{\mathrm{s}} + X_{\mathrm{sec}}$ [jΩ]	Coupling	R_{eq} [Ω]	X_{eq} [jΩ]
R2	8.41	0	5.3 %	3.32	0
R3	8.41	0	7.9 %	7.37	0
RC32	8.41	−5.19	5.3 %	2.44	1.46
RC33	8.41	−5.19	7.9 %	5.41	3.25
RL42	8.41	4.46	5.3 %	2.62	−1.35
RL43	8.41	4.46	7.9 %	5.81	−3.01

B. Design and Construction of the Inverters

Zero-voltage-switching (ZVS) Class E, and most recently Class EF, inverters are commonly implemented when a high frequency current or voltage output is required. This single low-side switch family of inverters can achieve high efficiencies (>95 % in [4]) operating in the multi-MHz region. The topology of the Class EF inverter is shown in Fig. 4. The topology of the Class E differs in that the LC branch comprised of L_2 and C_2 is not utilised. The purpose of this LC branch is to better shape the voltage and current in the transistor and therefore achieve a higher power output capability for a particular switching device.

The load-independent Class EF inverter [11], implemented in [3]–[6], [12], has additional advantageous features: it achieves ZVS for the entire resistive load range (0 Ω-$R_{\mathrm{eq_{max}}}$) and outputs a sinusoidal current waveform that is independent of the resistive load.

In this experiment, we designed a Class E inverter and a load-independent Class EF inverter using a Gallium Nitride FET as the switching device (GS66504B by GaN Systems). The designed values for the inverters are presented in Table III and the duty cycle was set at 28 % for the Class EF inverter, and at 50 % for the Class E.

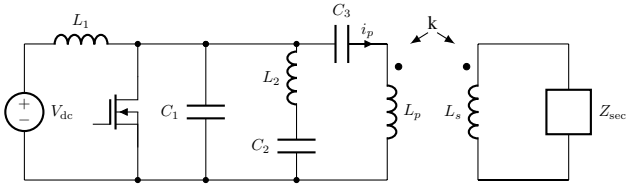

Fig. 4. Schematic a Class EF Inverter in an IPT system.

TABLE III
PASSIVE COMPONENT VALUES OF THE CANDIDATE INVERTERS

Design	L_1 [μH]	L_2 [nH]	C_1 [pF]	C_2 [pF]	C_3 [pF]
Class EF	88	267	156	176	130
Class E	88	-	81	-	163

C. Changing the Resistance and Reactance of an Inductively Powered Load

The inverters were first powered feeding a purely resistive load at various couplings, then a capacitive-resistive load and finally an inductive-resistive load. Measurements were taken for all cases in which the temperature of the transistor did not exceed 80 °C. The input power was measured for each of the previously characterised loads. The results are presented in Table IV. The drain voltage waveforms for both inverters under reactive and resistive loads are presented in Fig. 5, and Fig. 6 shows the experimental set-up for these measurements.

TABLE IV
INPUT POWER AT THE INVERTER [W]

Inverter	No load	R2	R3	RC32	RC33	RL42	RL43
Class E	14.4	63.6	108.0	52.8	109.2	49.2	81.6
Class EF	13.2	84.0	162.0	61.2	-	66.0	-

The effects of varying the resistive loads in Class E inverters and load-independent Class EF inverters are well known [11], [13], and the effects of a reflected reactance can be considered as a variation in C_3, i.e. the inverter being detuned. Interestingly for IPT, if the load has a fixed residual reactance, the reflected resistance and reactance both change as k changes. Therefore, the effects of a slightly detuned load moving across a charging pad affects both R_{eq} and X_{eq} gradually, depending on the phasor angle between the resistive load and the residual reactance. These effects can be appreciated on the drain voltage waveforms for each inverter in Fig. 5.

The load-independent Class EF inverter here presented was designed to tolerate resistive loads from 0 to 7 Ω and the Class E inverter can tolerate values larger than this (0 to 10 Ω) but with the disadvantage of having sub-optimum operation (the transistor's anti-parallel diode conducting) when the reflected resistive load is not equal to the maximum load. When a capacitive load is reflected to the transmitter (loads RL42 and

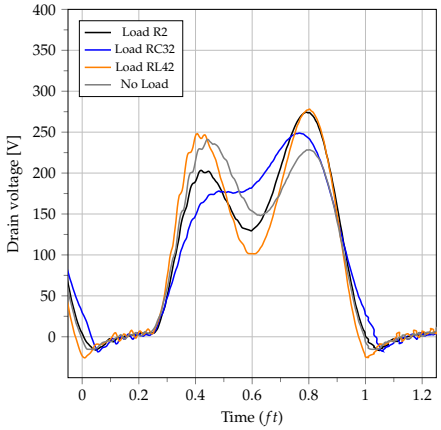

(a) Load-independent Class EF

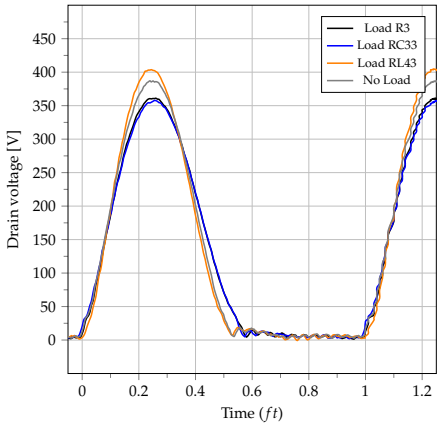

(b) Class E

Fig. 5. Oscilloscope drain voltage waveforms of the inverters handling resistive and reactive loads.

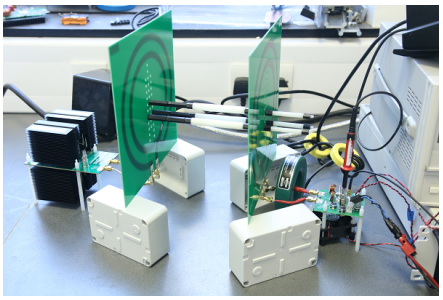

Fig. 6. Photograph of IPT experimental set-up.

RL43) both inverters tend to enter non-optimum operation. Interestingly, on the Class E the drain voltage waveform is similar to that of the unloaded condition. When an inductive load was reflected to the transmitter (RC32 and RC33) the load-independent Class EF loses the ZVS condition, while the Class E inverter shows a similar behaviour to that of a purely resistive reflected load.

IV. Conclusions

A detailed characterisation was performed on an IPT-link to assess and compare circuits used in multi-MHz IPT Systems. An application of the developed IPT-link is presented in this paper where an experimental comparison of a Class E inverter and a load-independent Class EF inverter handling resistive and reactive loads is shown for the first time.

Acknowledgement

The authors would like to acknowledge the following funding sources: the Department of Electrical and Electronic Engineering of Imperial College London, PINN Programme by the Ministry of Science and ICT of Costa Rica MICITT, University of Costa Rica and EPSRC grant ref: EP/R004137/1 Converter Architectures.

References

[1] S. I. Babic and C. Akyel, "Calculating mutual inductance between circular coils with inclined axes in air," *IEEE Trans. Magn.*, vol. 44, no. 7, pp. 1743–1750, July 2008.

[2] A. Tejeda, C. Carretero, J. T. Boys, and G. A. Covic, "Ferrite-less circular pad with controlled flux cancelation for ev wireless charging," *IEEE Trans. on Power Electron.*, vol. 32, no. 11, pp. 8349–8359, Nov 2017.

[3] A. Pacini, A. Costanzo, S. Aldhaher, and P. D. Mitcheson, "Load- and position-independent moving MHz WPT system based on GaN-distributed current sources," *IEEE Trans. Microw. Theory Techn.*, vol. 65, no. 12, pp. 5367–5376, Dec 2017.

[4] J. M. Arteaga, S. Aldhaher, G. Kkelis, D. C. Yates, and P. D. Mitcheson, "Multi-MHz IPT systems for variable coupling," *IEEE Trans. Power Electron.*, vol. PP, no. 99, pp. 1–1, 2017.

[5] S. Aldhaher, P. D. Mitcheson, J. M. Arteaga, G. Kkelis, and D. C. Yates, "Light-weight wireless power transfer for mid-air charging of drones," in *11th European Conf. on Antennas and Propagation (EUCAP)*, March 2017, pp. 1–5.

[6] G. Kkelis, S. Aldhaher, J. M. Arteaga, D. C. Yates, and P. D. Mitcheson, "Hybrid class-e synchronous rectifier for wireless powering of quad-copters," in *IEEE Wireless Power Transfer Conf. (WPTC)*, May 2017, pp. 1–4.

[7] G. Kkelis, D. C. Yates, and P. D. Mitcheson, "Class-E half-wave zero dv/dt rectifiers for inductive power transfer," *IEEE Trans. Power Electron.*, vol. PP, no. 99, pp. 1–1, 2017.

[8] A. A. Bastami, A. Jurkov, P. Gould, M. Hsing, M. Schmidt, J. I. Ha, and D. J. Perreault, "Dynamic matching system for radio-frequency plasma generation," *IEEE Trans. on Power Electron.*, vol. 33, no. 3, pp. 1940–1951, March 2018.

[9] W. B. Kuhn and A. P. Boutz, "Measuring and reporting high quality factors of inductors using vector network analyzers," *IEEE Trans. Microw. Theory Techn.*, vol. 58, no. 4, pp. 1046–1055, 2010.

[10] K. Van Schuylenbergh and R. Puers, *Inductive powering: Basic theory and application to biomedical systems*. Springer Science & Business Media, 2009.

[11] S. Aldhaher, D. C. Yates, and P. D. Mitcheson, "Load-independent class E/EF inverters and rectifiers for MHz-switching applications," *IEEE Trans. on Power Electron.*, pp. 1–1, 2018.

[12] J. M. Arteaga, S. Aldhaher, G. Kkelis, D. C. Yates, and P. D. Mitcheson, "Design of a 13.56 MHz ipt system optimised for dynamic wireless charging environments," in *2016 IEEE 2nd Annual Southern Power Electronics Conference (SPEC)*, Dec 2016, pp. 1–6.

[13] M. K. Kazimierczuk and D. Czarkowski, *Resonant power converters*. John Wiley & Sons, 2012.